



Solar cycle variation of the ionization by cosmic rays in the atmosphere at the mid-latitude region of Athens

P. Makrantonis¹ · H. Mavromichalaki¹ · P. Paschalis¹

Received: 30 May 2021 / Accepted: 12 July 2021
© The Author(s), under exclusive licence to Springer Nature B.V. 2021

Abstract In this study, the ionization rate in the atmosphere induced by solar and galactic cosmic rays is calculated for the region of Athens (Greece) during the time period from 1996 to 2019 covering the last two solar cycles 23 and 24. In order to compute the cosmic ray induced ionization, the corresponding model of the University of Oulu was used along with its new version which is extended to the upper atmosphere. This model has been applied to the entire atmosphere, i.e., from the atmospheric depth of 0.00 g/cm² corresponding to the upper limit of the atmosphere (~40 km), to that one of 1025 g/cm² corresponding to the Earth's surface. Furthermore, an application has been made as a function of rigidity and geomagnetic latitude, from 0.1 GV (~90° polar regions) to 14.9 GV (~0° equatorial regions). Specifically, we focus at the region of Athens that is a middle latitude one, located at 38°N geographic latitude, and cosmic ray intensity is recorded by the sea level (260 m) neutron monitor station of the National and Kapodistrian University of Athens. Cosmic ray particles with a vertical cut-off rigidity of 8.5 GV are measured in real time and magnetospheric effects of the cosmic ray intensity with the maximum amplitude in the north hemisphere, are often observed. A comparison of the calculated cosmic ray induced ionization in this region with the ionization of polar and equatorial regions during the different phases of the solar cycles 23 and 24, is performed. A seasonal variation of this ionization during all the examined period is for first time observed. Obtained results are discussed in terms of Space Weather applications.

Keywords Cosmic rays · Ionization · Atmosphere · Solar cycle · Neutron monitors

✉ H. Mavromichalaki
emavromi@phys.uoa.gr

¹ Nuclear and Particle Physics Section, Faculty of Physics, National and Kapodistrian University of Athens, Athens, Greece

1 Introduction

As it is known the ionization of the atmosphere is a significant factor affecting the physical-chemical composition of the entire atmosphere (Dorman 2004; Harrison and Tammet 2008) and thus several climate parameters, such as precipitation, cyclogenesis, cloud cover in mid- to high-latitude regions, atmospheric transparency and aerosol formation (Bazilevskaya et al. 2008). Cosmic rays are the main ionizing agent for lower and middle atmosphere and for practical purposes, such as for the impact of cosmic radiation on the cloud formation and the ozone layer, it is of high importance to calculate precisely the Cosmic Ray Induced Ionization (CRII) and its variations according to time, location, solar and geomagnetic activity (Usoskin et al. 2009a). The CRII depends on two main factors: the solar activity that modulates the intensity of the cosmic ray flux and the geomagnetic field that acts as a charged particle discriminator and determines which particles arrive at the Earth at the different latitudes.

Both high energy galactic cosmic rays (GCR), always present in the vicinity of the Earth and affected by solar modulation, and sporadic solar energetic particles (SEPs) of lower energy but high peak flux, are the major components for CRII (Usoskin et al. 2009a). Besides the permanent flux of GCR, sporadic SEP events may occur when, due to solar flares or CMEs, strong fluxes of energetic particles are produced. Such particles (mostly protons), when they interact with the Earth's atmosphere, produce a significant increase of the atmosphere's ionization (Schröter et al. 2006). SEPs are mostly accelerated up to hundreds MeV, thus the respective increase of ionization is observed only in the polar atmosphere at high altitude. Nevertheless, during strong events called ground level enhancement of cosmic rays (GLE), particles may be accelerated up to a few GeV.

Consequently, GLEs can cause ionization effects even to the lower altitudes. More to that, it is shown that the direct ionization effect by GLEs is negligible or even negative in all low and mid-latitude regions, because of the accompanying Forbush decreases. Only in polar atmosphere the effect is positive where, during major GLE events, it can be dramatic in the upper atmosphere (Usoskin et al. 2009b).

The cosmic ray ionization can be satisfactorily computed by some numerical models (Usoskin et al. 2009a). In this work, the CRII model of the University of Oulu applied to the entire atmosphere (Usoskin and Kovaltsov 2006; Usoskin et al. 2010) has been used for ionization calculations at three specific latitudes (polar, mid-latitude and equatorial regions) for different time periods during the solar cycles 23 and 24. A comparison among these regions with different cut-off rigidities and time periods during the different phases of the solar cycles gives significant conclusions useful for space weather applications. A more extended study is performed for the middle latitude region of Athens in Greece using data from the Athens Neutron Monitor Station.

2 Data selection

In order to calculate the CRII for specific time periods, latitudes and altitudes, the “Cosmic Ray Induced Ionization: Do-it-yourself kit” (<http://cosmicrays.oulu.fi/CRII/CRII.html>) of the Oulu Cosmic Ray Station has been used. In this kit, recalculated tables of cosmic ray induced ionization (CRII) in units of ion pairs/g/sec are given. Each table concerns a specific residual atmospheric depth starting from 0.00 g/cm² to 1025 g/cm². In the first line of each table, one finds the values of the modulation potential Φ in MV (from 0 to 1500 MV), whereas the following lines give the geomagnetic cut-off rigidity R_c in GV (first number), followed by the CRII for the corresponding values of R_c (raw) and Φ (column).

Monthly and annual values of the modulation parameter Φ (in MV) reconstructed from the ground based cosmic ray data, can be found at <http://cosmicrays.oulu.fi/phi/phi.html> in tabular and vector form (Usoskin et al. 2005, 2011). The modulation parameter corresponds to the local interstellar spectrum (LIS) of cosmic rays as provided by Burger et al. (2000).

Regarding the cosmic ray intensity data at the region of Athens, they were obtained from the Athens Neutron Monitor Station – A.Ne.Mo.S (<http://cosray.phys.uoa.gr>) of the National and Kapodistrian University of Athens in Greece operating from the year 2000 in real time mode. It is a middle latitude station with geographic coordinates 38°N and 24°E and cut-off rigidity equal to 8.5 GV. It is located at an altitude of 260 m above sea level. It is the unique station in the Balkan and East Mediterranean region covering the cut-off rigidities from 6.34 GV (Rome) to 11.9 GV (Tel-Aviv).

This station provides the possibility studying ionization effects by cosmic rays and consequently climate variability in these regions.

As it concerns the Sunspot Number, data of “Sunspot Index and Long-term Solar Observations” of the Royal Observatory of Belgium (<http://www.sidc.be/silso/datafiles#total>) are used.

3 The CRII model

The CRII model is a numerical model that calculates the cosmic ray induced ionization in the entire atmosphere from the ground up to approximately 40 km of altitude, all over the globe. The model computations coincide with direct fragmentary measurements of the atmospheric ionization in a full range of parameters, covering all latitudes and altitudes during different solar cycle phases confirming its reliability and validity.

In this model the Monte Carlo CORSIKA tool is used (v.6.617 August 2007) (Heck et al. 1998), which provides a full development simulation of an electromagnetic-muon-nucleonic cascade in the atmosphere, as well as the FLUKA package for the low-energy interactions (v.2006.3b March 2007) (Fassò et al. 2001). The results of these simulations are presented in tables, as the ionization yield function (Y). This function (Y) shows the number of ion pairs that are produced per gram of ambient air at a specific atmospheric depth, by one nucleon of primary CR particle with the energy per nucleon given (ion pairs sr cm² g⁻¹).

The energy spectrum of the primary incoming cosmic rays (both solar and galactic), which fundamentally consist of α -particles and protons, is considered to be known. The parametrized differential energy spectrum of galactic cosmic rays at the Earth’s orbit is given by the force field model (Gleeson and Axford 1968; Caballero-Lopez and Moraal 2004; McCracken and Beer 2007). The modulation potential (ϕ given in MV) provides a good single-parameter approximation of the actual shape of the cosmic ray spectrum near Earth (Usoskin et al. 2005). An implicit parameter of the force field approximation is the shape of the LIS, which is not well known. In this model, the LIS for protons in line with Burger et al. (2000) is used. Regarding the heavier species, since they are identical to α -particles, both in the induced ionization and in the heliospheric modulation ($Z/A \approx 1/2$), all the nuclei heavier than protons are considered as α -particles with the corresponding number of nucleons. The heavier nuclei (including α -particles) to protons ratio is defined to be 0.3 in the interstellar space (e.g., Gaisser et al. 2013).

The CRII rate (number of ion pairs produced in one gram of the ambient air per second) at a specific atmospheric

depth x can be represented in as follows:

$$Q(x, \phi) = \sum_i Q_i = \sum_i \int_{T_{c,i}}^{\infty} J_i(T, \phi) \cdot Y_i(x, T) \cdot dT$$

where $J_i(T, \phi)$ is the differential energy spectrum of galactic cosmic rays in the Earth's vicinity (in units of $[\text{cm}^2 \text{ sec sr} (\text{GeV/nuc})]^{-1}$), $Y_i(x, T)$ is the ionization yield function (number of ion pairs produced at the atmospheric depth x by one primary cosmic ray particle of the i -th type, isotropically impinging on the Earth's magnetosphere with kinetic energy T), and the summation is carried out over different i -th species of CR (α -particles, protons, heavier species). Integration is carried out above $T_{c,i}$, which is the kinetic energy of an i -th type particle, corresponding to the local geomagnetic cut-off rigidity R_c . The full details of the CRII model are given in Usoskin and Kovaltsov (2006) and Usoskin et al. (2010).

4 Results

Using the CRII model of Usoskin and Kovaltsov (2006) and the extension of this of Usoskin et al. (2010), a study of the distribution of ionization on a monthly and yearly basis during the solar cycles 23 and 24 covering the years from 1996 to 2008 and from 2009 to 2019 respectively, was performed. These cycles are characterized by different features, being the first one as a cycle with intense solar activity and the second one being a very calm cycle. Generally, a gradual increase of the ionization rate from the solar maximum to the solar minimum, and vice versa, was observed. However, it is noted that this gradual increase is disturbed when the solar activity is greater than that during the solar maximum of the respective cycle, i.e., comparing the year 2001 with the years 2000 and 2003 of the solar cycle 23. Finally, a seasonal variation of the CRII is observed, with a few deviations due to strong solar activity.

4.1 Yearly distribution of the CRII

Applying the CRII model in the entire atmosphere, we have calculated the ionization induced by cosmic rays in each year of the two solar cycles 23 and 24. These calculations have been done for a polar region, a middle latitude and an equatorial region as well as during the minima, ascending/descending phases and solar maxima of these cycles. Some indicative results are given in the following figures.

The cosmic ray induced ionization at the solar maxima (year 2001 for the cycle 23 and year 2014 for the cycle 24) and at the solar minima (year 1996 for solar cycle 23 and year 2009 for the solar cycle 24), for a Polar region ($R_c = 0.1$ GV), for a middle latitude region (Athens, $R_c = 8.5$ GV), and for an Equatorial region ($R_c = 14.9$ GV), as

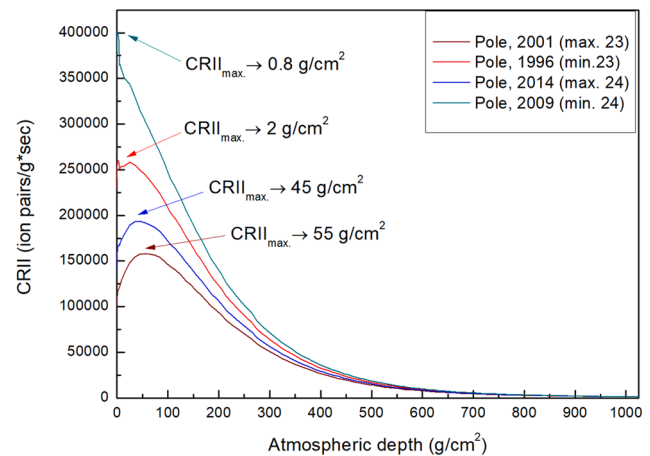


Fig. 1 Distribution of the CRII as a function of the atmospheric depth at Polar regions (cut-off rigidity 0.1 GV), during the years 1996 and 2001 (solar minimum and maximum of solar cycle 23, respectively) and the years 2009 and 2014 (solar minimum and maximum of solar cycle 24, respectively)

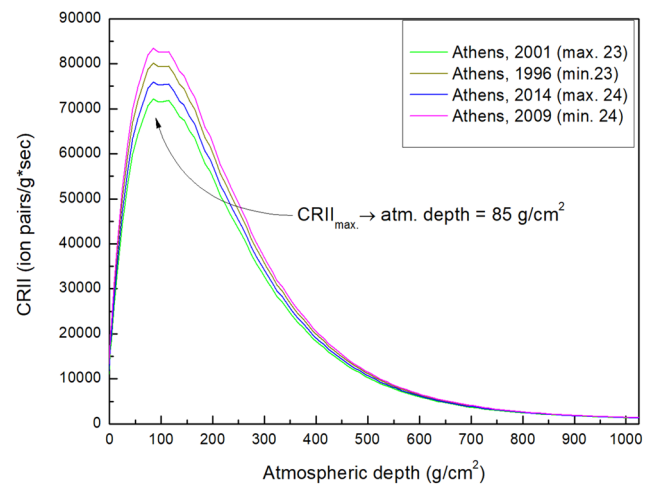


Fig. 2 Distribution of the CRII as a function of atmospheric depth at Athens region (cut-off rigidity 8.5 GV), during the solar maximum and minimum of the solar cycles 23 and 24

a function of the atmospheric depth, is presented in Figs. 1, 2, 3, respectively. It is obvious that during the solar maxima (2001, 2014), the ionization presents minimum values, while during the solar minima (1996, 2009), the ionization is maximum. More to that, we observe that the CRII has the minimum values when the solar activity is greater than the one during the solar maximum of the respective cycle, i.e., comparing year 2001 with years 2000 and 2003. This indicates that the ionization follows the behavior of the cosmic rays, which is negatively correlated with the solar activity (Forbush 1954).

Observing Table 1, it is important to mention that, regarding the solar cycle 23, during the solar maximum, the ionization is almost two times greater at the Poles than in

Table 1 Maximum values of CRII during the solar minimum and maximum of solar cycles 23 and 24, at a Polar region ($R_c = 0.1$ GV), a middle latitude region (Athens, $R_c = 8.5$ GV), and an Equatorial region ($R_c = 14.9$ GV)

YEARS	CRII (ion pairs/g*sec)		
	Polar Region 0.1 GV	Mid-Latitude Region Athens 8.5 GV	Equatorial Region 14.9 GV
1996 (min. SC23)	260.10 ³ (2 g/cm ²)	80.10 ³ (85 g/cm ²)	51.10 ³ (115 g/cm ²)
	258.10 ³ (25 g/cm ²)	80.10 ³ (115 g/cm ²)	
2009 (min. SC24)	402.10 ³ (0.8 g/cm ²)	84.10 ³ (85 g/cm ²)	53.10 ³ (115 g/cm ²)
		83.10 ³ (115 g/cm ²)	
2001 (max. SC23)	158.10 ³ (55 g/cm ²)	72.10 ³ (85 g/cm ²)	48.10 ³ (115 g/cm ²)
		72.10 ³ (115 g/cm ²)	
2014 (max. SC24)	194.10 ³ (45 g/cm ²)	76.10 ³ (85 g/cm ²)	50.10 ³ (115 g/cm ²)
		75.10 ³ (115 g/cm ²)	

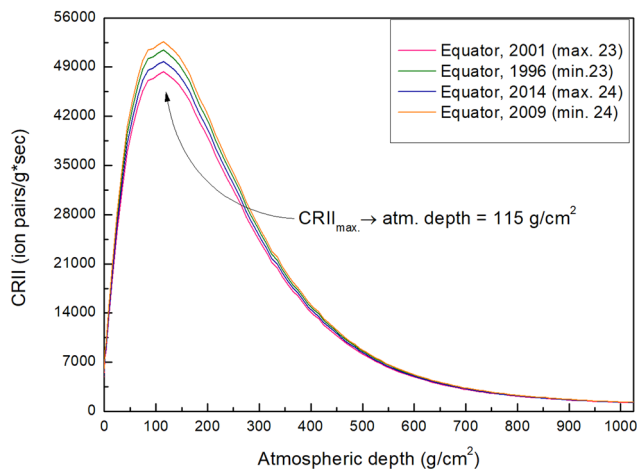


Fig. 3 Distribution of the CRII as a function of atmospheric depth, at Equatorial regions (cut-off rigidity 14.9 GV), for the solar maximum and minimum of the solar cycles 23 and 24

Athens, while during the solar minimum, it is almost three and a half times greater. Especially, regarding the solar cycle 24, during the solar maximum, the ionization is two and a half times greater at the Poles than in Athens, while during the solar minimum, it is almost five times greater!

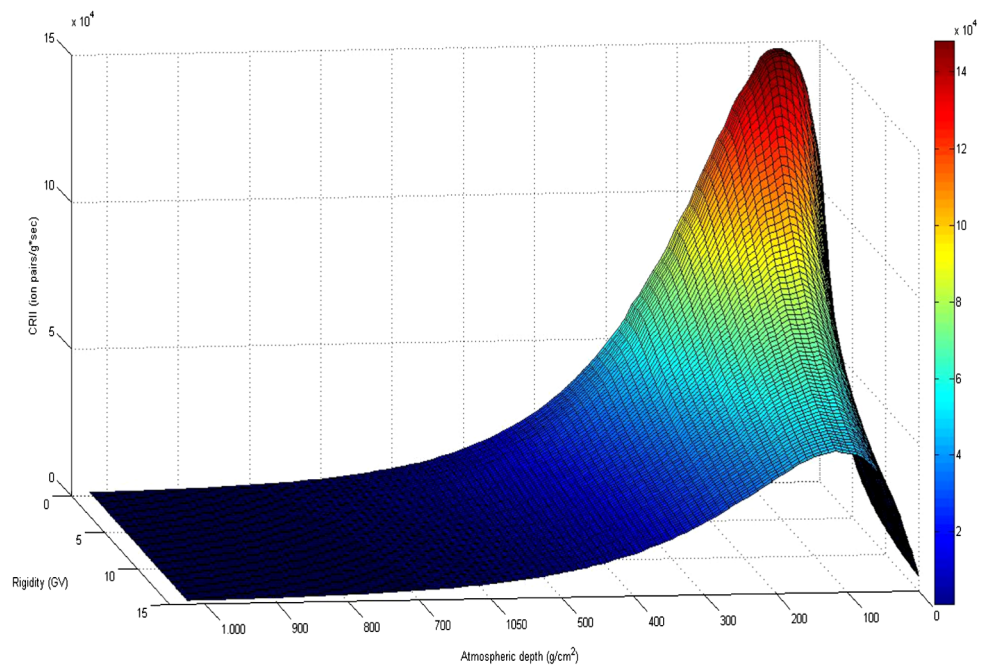
Respectively, regarding the solar cycle 23, during the solar maximum, the ionization is almost three times greater at the Polar than in the Equatorial regions, while during the solar minimum, it is almost five times greater. Regarding the solar cycle 24, during the solar maximum, the ionization is almost four times greater at the Polar than in the Equatorial regions, while during the solar minimum, it is almost seven and a half times greater! This should be due to the fact that

the solar cycle 24 was generally a quiet cycle in comparison with the solar cycle 23 that was very active and thus the CRII had greater fluctuations and greater values during the solar cycle 24. Comparing the respective values between Athens and Equatorial regions, we note that the variation is slightly bigger during the solar cycle 24, which confirms that solar activity has greater impact on the CRII at low rigidity areas. However, we still have greater CRII values during the last solar cycle.

Furthermore, we observe that for the region of Athens there is a double peak, one at the atmospheric depth 85 g/cm² and one at 115 g/cm², with the 85 g/cm² to be the biggest one, while for the Equatorial region, we note there is one peak at the 115 g/cm². For the Polar regions, the ionization rate is maximum at lower, unpredictable atmospheric depths. As it concerns the Polar regions, we also note that during the solar maxima the ionization curve is smooth with one maximum value at different atmospheric depths though, whereas during the solar minimum 2009 it has one peak at very low atmospheric depth (0.8 g/cm²) and during the solar minimum 1996 there is a double peak, one at the atmospheric depth of 2 g/cm² and one at 25 g/cm², with the value of 2 g/cm² to be the biggest one.

It is noted that the atmospheric depths of 85 and 115 g/cm² (~100 g/cm²) roughly correspond to the altitude of 18–20 km, where the secondary energetic particles are generated. Thus, as we go toward the Poles, maximum CRII ionization is found to be in lower atmospheric depths, i.e., higher in the atmosphere, and during the minimum of the solar cycles, the ionization rate is growing, and the difference between the ionization rate during the maximum and the minimum of solar cycle in each location, is significantly increased.

Fig. 4 Three-dimensional presentation of the annual distribution of CRII as a function of cut-off rigidity (GV) and atmospheric depth (g/cm^2), for the year 2000, when solar activity was very intense during the solar cycle 23



All this is due to the geomagnetic cut-off rigidity of each location (R_c), as the lower it is, the more cosmic rays enter the magnetosphere and the atmosphere, which then can ionize it and create different effects (Gerontidou et al. 2021).

All of the above are shown indicatively in Fig. 4 where the annual distribution of CRII is depicted three dimensionally as a function of cut-off rigidity and atmospheric depth, for the year 2000, when solar activity was very intense during the solar cycle 23. It is obvious, once again, that for rigidities around 0 GV, i.e., Polar regions, the ionization rate is maximum at lower atmospheric depths (higher altitude), while as we move toward rigidities 15 GV, i.e., Equatorial regions, the maximum ionization rate is fixed approximately at $100 \text{ g}/\text{cm}^2$ (18–20 km altitude) where the production of muons from the cosmic ray particles is maximum.

Moreover, it is resulted that the solar cycle 24 is a quiet and less active solar cycle, thus we notice that in general the ionization rates during the solar maximum and minimum are higher than the ones during the solar cycle 23.

4.2 Long term modulation of the CRII

It is known that the atmospheric depth of $x = 700 \text{ g}/\text{cm}^2$ ($\sim 3 \text{ km}$ altitude) is useful for the comparison with the formation of low clouds (Bazilevskaya et al. 2008). Thus, time profiles of monthly values of the calculated CRII from the year 1996 to the year 2019, covering two solar cycles, at the atmospheric depth of $x = 700 \text{ g}/\text{cm}^2$ ($\sim 3 \text{ km}$ altitude) are illustrated in Fig. 5 for polar (upper curve), mid-latitude (middle curve) and equatorial (lower curve) regions. It is important to be noted that the ionization rate presents a long-

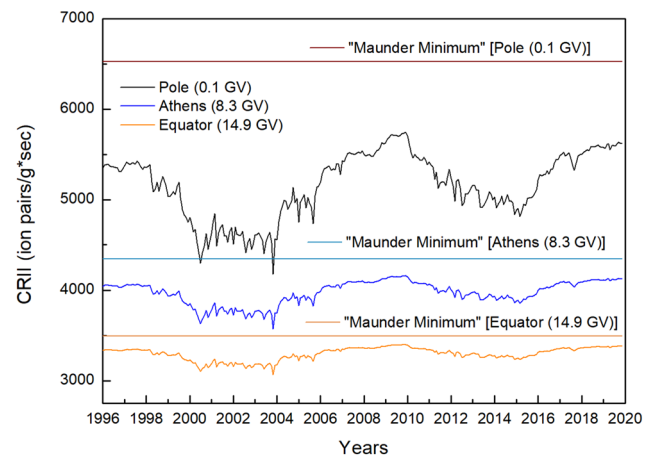


Fig. 5 Time profiles of the monthly distribution of CRII at the atmospheric depth $x = 700 \text{ g}/\text{cm}^2$ ($\sim 3 \text{ km}$ altitude), at the Polar (0.1 GV) (upper curve), Athens (8.5 GV) (middle curve) and Equatorial region (14.9 GV) (lower curve), for the time period 1996–2019, illustrating the ionization effect of CRs if there was no solar modulation, i.e., $\phi = 0$, which would roughly correspond to the “Maunder minimum” of solar activity

term modulation that means an 11-year variation, similar to that one of the galactic cosmic ray intensity at all the above regions (Mavromichalaki et al. 1995). This effect is known that it is due to the solar activity and is more intense in the Polar Regions. In addition, a possible comparison of the actual calculated ionization for the Poles, the Equator and the Athens to the “Maunder Minimum” period that is characterized from the lack of solar activity, is also presented in this figure (Bazilevskaya et al. 2008; Usoskin et al. 2010).

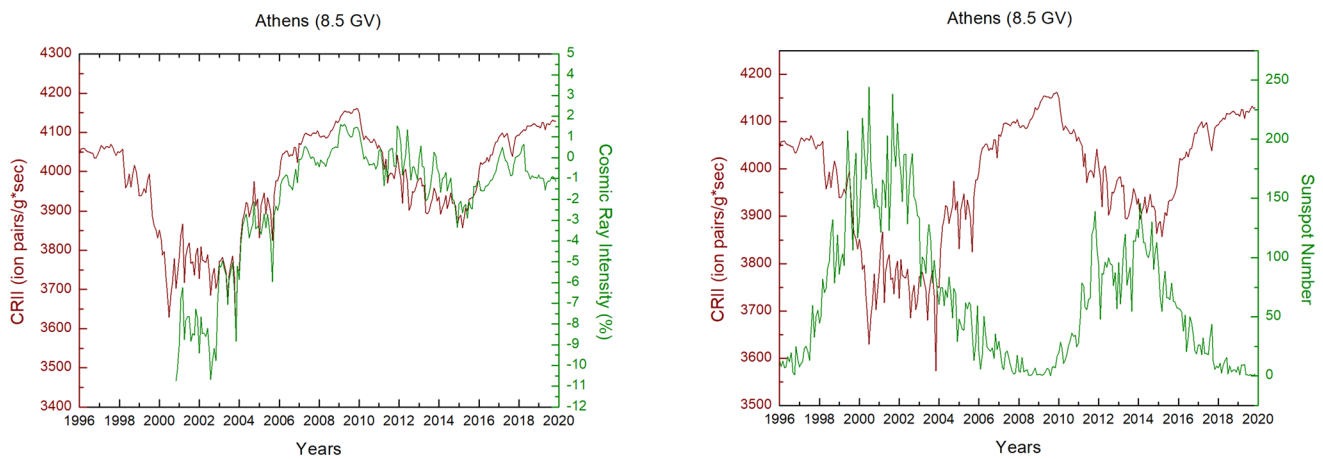


Fig. 6 Comparison of the monthly distribution of CRII at the atmospheric depth $x = 700 \text{ g/cm}^2$ (red line, both panels), with the cosmic ray intensity of the Athens Neutron Monitor (green line, left panel) and the sunspot number (green line, right panel) for the time period 1996-2019

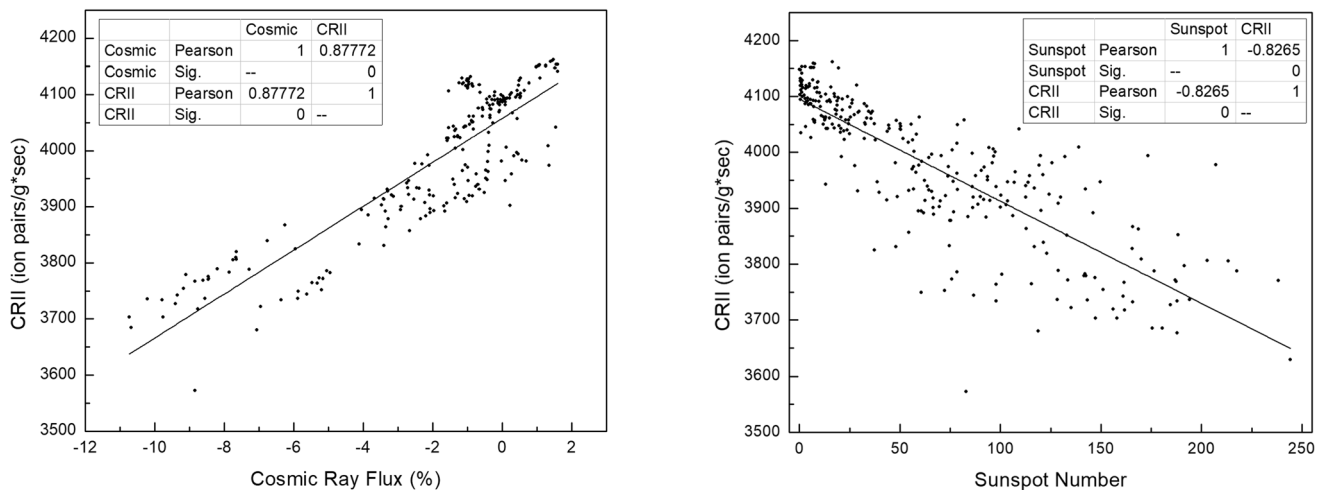


Fig. 7 Correlation between the monthly distribution of CRII at the atmospheric depth $x = 700 \text{ g/cm}^2$ and the cosmic ray intensity of the Athens Neutron Monitor for the time period 2000-2019 (left panel), and the sunspot number (right panel), for the time period 1996-2019

4.3 Cosmic ray intensity and solar activity

A comparison of the distribution of CRII, at the atmospheric depth of $x = 700 \text{ g/cm}^2$, to the cosmic ray flux recorded by the Athens Neutron Monitor, during the solar cycles 23 and 24, was performed on a monthly basis, and it is illustrated in Fig. 6 (left panel). We observe that CRII is in a positive correlation with the intensity of the cosmic ray flux, while a negative correlation with solar activity, expressed by the sunspot number, is obvious too (Fig. 6, right panel). In Fig. 7, the exact correlation between the monthly distribution of CRII and the cosmic ray intensity of the Athens Neutron Monitor for the time period 2000-2019 is shown in the left panel (Pearson correlation coefficient 0.88), whereas the correlation between the monthly distribution of CRII and the sunspot number, for the time period 1996-2019, is shown in the right panel (Pearson correlation coefficient -0.83).

It is concluded from this analysis that the ionization rate due to cosmic rays follow well the behavior of the cosmic ray intensity measured by ground-based detectors presenting an 11-year cycle, while the solar activity expressed by the sunspot number, is in inverse relation with it (Forbush 1954; Makrantoní et al. 2013).

4.4 Seasonal variation of the CRII

The monthly distribution of the calculated CRII in Athens for the solar cycles 23 and 24, at atmospheric depth 100 g/cm^2 , where the maximum ionization in the atmosphere is observed, are presented in Figs. 8 and 9 respectively. Actually, we noted that at the region of Athens we have the maximum ionization at atmospheric depth 85 g/cm^2 and a second peak at 115 g/cm^2 ; thus, for this monthly distribution, the mean CRII of these two atmospheric depths is used.

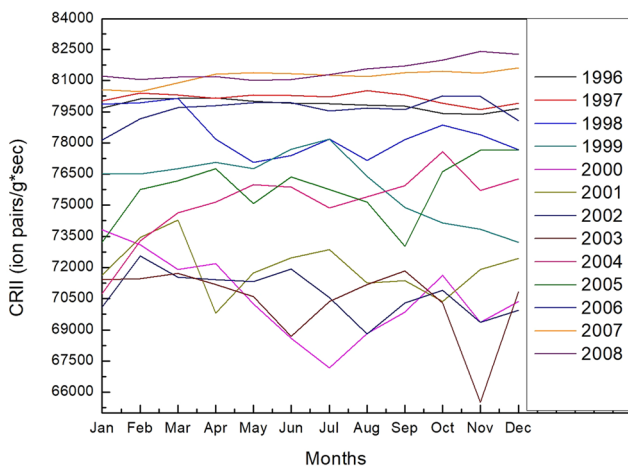


Fig. 8 Seasonal variation of CRII at the atmospheric depth $x = 100$ g/cm^2 (~ 18 - 20 km altitude), in Athens (8.5 GV), for each year of the solar cycle 23

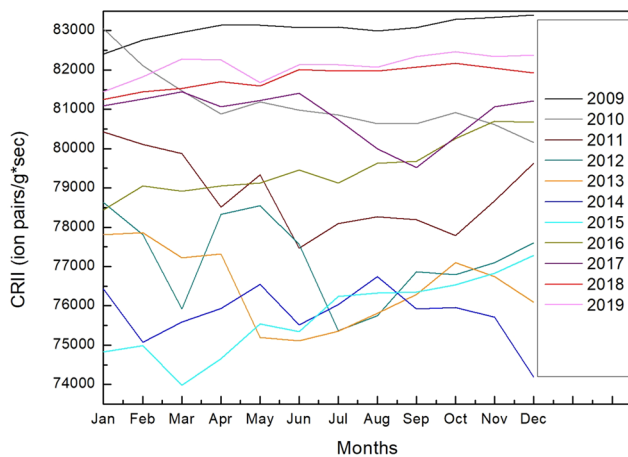


Fig. 9 Seasonal variation of CRII at the atmospheric depth $x = 100$ g/cm^2 , in Athens (8.5 GV), for each year of the solar cycle 24

With these graphs we would like to study whether there is a seasonal variation of the Cosmic Ray Induced Ionization.

The monthly distribution of CRII for each year of the solar cycle 23, is presented in Fig. 8. In this graph, we can clearly distinguish the different solar cycle phases. On the top, we have the years during which we had minimum solar activity (2008, 2007, 1997, 1996, 2006), in the middle the years that correspond to the ascending and descending phases of the solar cycle (1995, 1999, 2005, 2004) and at the bottom we have the years that correspond to maximum solar activity (2001, 2002, 2003, 2000).

Since the solar cycle 24 is generally characterized by low solar activity, we can see in Fig. 9 that there is not such a clear distinction between the solar phases as there is for solar cycle 23. However, it is clear enough that the same pattern is followed on the top of the graph, we have the years during which we had minimum solar activity (2009, 2019,

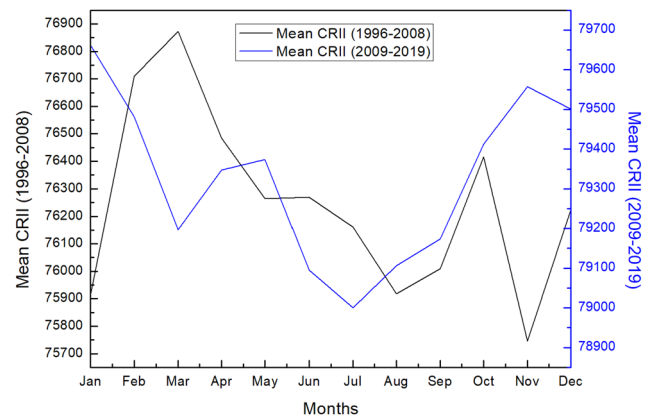


Fig. 10 Comparison of seasonal variation of the mean CRII of solar cycle 23 (black line) and solar cycle 24 (blue line), at the atmospheric depth $x = 100$ g/cm^2 in Athens (8.5 GV)

2018), a little lower we find the years that correspond to the ascending and descending phases of this solar cycle (2010, 2017, 2016, 2011), and as we go downwards, we meet the years where there was maximum solar activity (2012, 2013, 2014, 2015). The more active the Sun is, the more obvious the solar phases are.

The calculated mean monthly CRII over the solar cycle 23 (black line) and the corresponding one of the solar cycle 24 (blue line) are illustrated in Fig. 10. We note that the mean CRII line of solar cycle 23 present sharp peaks, as it was a very active solar cycle; whereas the mean CRII line of solar cycle 24, where there was lower solar activity, is smoother. Nevertheless, it is obvious in both cases that there is a seasonal variation of the Cosmic Ray Induced Ionization for both cycles. More specifically, the seasonal variation of the CRII is in an absolute negative correlation between the two solar cycles for the seasons March-April and October-November, during which strong solar activity was recorded, such as the events of October 2003, of March 2012, etc. (Papaioannou et al. 2010; Plainaki et al. 2005; Livada et al. 2018).

5 Conclusions

In this work the 11-year modulation of the ionization rate induced by cosmic rays in the entire atmosphere using the CRII model, was studied. From the detailed analysis of this atmospheric ionization at Polar, Mid and Equatorial regions on monthly and yearly basis during the time period 1996 to 2019, covering two solar cycles, we have concluded the following:

The CRII model is an important tool providing the opportunity to compute the cosmic ray induced ionization in the entire atmosphere for desired locations and for different conditions. Comparing the CRII calculations to the mea-

sured cosmic ray intensity data recorded at the neutron monitor station operated at the University of Athens, a sea level and middle latitude station, during the two solar cycles 23 and 24, satisfactory results useful for the Space Weather and Climate community are obtained (Makrantoní et al. 2013; Bazilevskaya and Mironova 2015; Christodoulakis et al. 2019).

Estimating the ionization induced by the cosmic rays in this middle latitude region, it seems to have different values during the minimum, ascending /descending and maximum phases of each one of these cycles, being greater during the minimum phase of them.

It is also reported that the ionization values in these two cycles present differences as well as in the polar and equatorial regions with the greater ones during the solar cycle 24 that is a quieter cycle. Possibly this is resulting from the fact that the examined time interval includes an even and an odd solar cycle that follow the behavior of the 22-year variation of cosmic ray activity due to the polarity reversal of the solar magnetic field in the maximum periods (Mavromichalaki et al. 1997).

In general, the CR_{II} values are more intense in the polar regions, while in the middle and equatorial regions the CR_{II} values present only small differences in the maximum and minimum periods. It is also outlined from Fig. 5, where the CR_{II} during the Maunder minimum are presented. It is concluded that the solar activity is an important factor to the ionization production by the cosmic rays that are strongly modulated by this activity.

Moreover, studying the distribution of the ionization on Earth for several cut-off rigidities ranged from 0.1 to 14.9 GV, that means for geomagnetic latitudes 0°–90°, as it was expected, we note that there is a maximum value of ionization at Polar region, during the solar minima, for the most rigidities roughly at the atmospheric depth of $x = 100$ g/cm², where the production of muons is maximum due to the interaction of the cosmic rays with the molecules of the atmosphere.

Finally, a seasonal variation of the ionization induced by the cosmic rays during the last two solar cycles 23 and 24 is for first time observed and differences among the phases of these cycles are determined. In opposite with the minima of the cycles 23 and 24, high variations are observed during the maxima and the ascending/descending phases of these solar cycles, as well as in the periods when the Sun is very active (e.g., during the “Halloween solar storms” that occurred from mid-October to early November 2003). The calculated ionization during the minima of the solar cycles seems not to be characterized by conspicuous seasonal variations.

All this strengthens the belief that variations in the cosmic ray intensity, measured by the ground-based neutron monitors, are a significant factor in the expecting ionization of the atmosphere and thus in impacting the Earth’s climate.

For example, a decrease of atmospheric ionization leads to a decrease in the concentration of charge condensation centres in which a decrease of total cloudiness and atmosphere turbulence together with an increase in isobaric levels is observed. As a result, a decrease of rainfall is also expected. Similarly, Todd and Kniveton (2001), investigating 32 Forbush decrease events over the period 1983–2000, found reduced cloud cover of 18% and 12% (Dorman 2016). During big solar CR events when CR intensity and ionization in the atmosphere significantly increases, an inverse situation is expected and an increase in cloudiness should lead to an increase in rainfall.

Concluding, we can say that a future investigation of the meteorological parameters and the climate factors in combination with the results of this work concerning the solar cycle variations of the cosmic ray intensity and consequently of the ionization rate in the atmosphere will lead for a better understanding of atmospheric and space weather conditions.

From our point of view, cosmic rays and induced ionization, through their influence on cloudiness, are important factors in understanding climate.

Acknowledgements Thanks are due to the Special Research Account of the University of Athens for supporting the Cosmic Ray research. Thanks are also due to the Oulu Cosmic ray colleagues for kindly providing cosmic ray data as well as the Cosmic Ray Induced Ionization model.

Conflict of interest The authors indicate that there is not conflict of interest.

Publisher’s Note Springer Nature remains neutral with regard to jurisdictional claims in published maps and institutional affiliations.

References

- Bazilevskaya, G.A., Mironova, I.A.: In: Earth’s Climate Response to a Changing Sun, p. 77. EDP Sciences. Ch. 2.3 (2015)
- Bazilevskaya, G.A., Usoskin, I.G., Flückiger, E.O., et al.: Space Sci. Rev. **137**, 149 (2008). <https://doi.org/10.1007/s11214-008-9339-y>
- Burger, R.A., Potgieter, M.S., Heber, B.: J. Geophys. Res. **105**(27), 447 (2000)
- Caballero-Lopez, R.A., Moraal, H.: J. Geophys. Res. **109**, A01101 (2004). <https://doi.org/10.1029/2003JA010098>
- Christodoulakis, J., Varotsos, C., Mavromichalaki, H., Eustathiou, M., Gerontidou, M.: J. Atmos. Sol.-Terr. Phys. **189**, 98 (2019). <https://doi.org/10.1016/j.jastp.2019.04.012>
- Dorman, L.: Cosmic Rays in the Earth’s Atmosphere and Underground. Kluwer Academic, Dordrecht (2004)
- Dorman, L.I.: Space weather and cosmic ray effects. In: Climate Change, p. 513 (2016). Chap. 30. <https://doi.org/10.1016/B978-0-444-63524-2.00030-0>
- Fassò, A., Ferrari, A., Sala, P.R.: Particle Transport Simulation and Applications p. 159 (2001)
- Forbush, S.E.: J. Geophys. Res. **54**, 52 (1954). <https://doi.org/10.1029/JZ059i004p00525>
- Gaisser, T.K., Stanev, T., Tilav, S.: Front. Phys. **8**, 748 (2013). <https://doi.org/10.1007/s11467-013-0319-7>

- Gerontidou, M., Mavromichalaki, H., Katsourakis, N., Eroshenko, E., Yanke, V.: *Adv. Space Res.* **67**, 2231 (2021). <https://doi.org/10.1016/j.asr.2021.01.011>
- Gleeson, L.J., Axford, W.I.: *Astrophys. J.* **154**, 1011 (1968). <https://doi.org/10.1086/149822>
- Harrison, R.G., Tammiet, H.: Ions in the terrestrial atmosphere and other solar system atmospheres. *Space Sci. Rev.* **137**, 107–118 (2008). <https://doi.org/10.1007/s11214-008-9356-x>
- Heck, D., Knapp, J., Capdevielle, J.N., Schatz, G., Thouw, T.: CORSIKA: a Monte Carlo code to simulate extensive air showers. FZKA 6019, Forsch. Karlsruhe, Germany (1998)
- Livada, M., Mavromichalaki, H., Plainaki, C.: *Astrophys. Space Sci.* **363**, 8 (2018). <https://doi.org/10.1007/s10509-017-3230-9>
- Makrantonis, P., Mavromichalaki, H., Usoskin, I.G., Papaioannou, A.: *J. Phys. Conf. Ser.* **409**, 2232 (2013). <https://doi.org/10.1088/1742-6596/409/1/012232>
- Mavromichalaki, H., Marmatsouri, L., Vassilaki, A.: *Astrophys. Space Sci.* **232**, 315 (1995)
- Mavromichalaki, H., Belehaki, A., Rafios, X.: *Astron. Astrophys.* **330**, 764 (1997)
- McCracken, K.G., Beer, J.: *J. Geophys. Res.* **112**, A10101 (2007). <https://doi.org/10.1029/2006JA012117>
- Papaioannou, A., Makrantonis, P., Mavromichalaki, H.: In: Tsiganos, K., et al. (eds.) 9th Hellenic Astron. Union Conference (Athens), 48, 2009. ASP Conference Series, vol. 424, p. 83 (2010)
- Plainaki, C., Belov, A., Eroshenko, E., Kurt, V., Mavromichalaki, H., Yanke, V.: *Adv. Space Res.* **35**, 691 (2005)
- Schröter, J., Heber, B., Steinhilber, F., Kallenrode, M.B.: *Adv. Space Res.* **37**, 1597 (2006). <https://doi.org/10.1016/j.asr.2005.05.085>
- Todd, M.C., Kniveton, D.R.: *J. Geophys. Res.* **106**(D23), 32031 (2001)
- Usoskin, I.G., Kovaltsov, G.A.: *J. Geophys. Res.* **111**, D21206 (2006). <https://doi.org/10.1029/2006JD007150>
- Usoskin, I.G., Alanko-Huotari, K., Kovaltsov, G.A., Mursula, K.: *J. Geophys. Res.* **110**, A12108 (2005). <https://doi.org/10.1029/2005JA011250>
- Usoskin, I.G., Desorgher, L., Velinov, P., Storini, M., Flueckiger, E.O., Buetikofer, R., Kovaltsov, G.A.: *Acta Geophys.* **57**, 88 (2009a). <https://doi.org/10.2478/s11600-008-0019-9>
- Usoskin, I.G., Tylka, A.J., Kovaltsov, G.A., Dietrich, W.F.: In: Proc. 31st Intern. Cosmic Ray Conf., Lodz, Poland, ID: icrc0162 (2009b)
- Usoskin, I.G., Kovaltsov, G.A., Mironova, I.A.: *J. Geophys. Res.* **115**, D10302 (2010). <https://doi.org/10.1029/2009JD013142>
- Usoskin, I.G., Bazilevskaya, G.A., Kovaltsov, G.A.: *J. Geophys. Res.* **116**, A02104 (2011). <https://doi.org/10.1029/2010JA016105>